Electronic Supplementary Material (ESI) for Inorganic Chemistry Frontiers.

Supporting Information

Compositing MXene with hierarchical ZIF-67/cobalt hydroxide via controllable in situ etching for high-performance supercapacitor

Chunli Liu[a], Wenhao Feng[a], Yang Bai[b,c], and Huan Pang[a,*]

[a] School of Chemistry and Chemical Engineering, Yangzhou University, Yangzhou, Jiangsu, 225009, P. R. China

[b] School of Pharmacy, Changzhou University, Changzhou, Jiangsu, 213164, P. R. China

[c] State Key Laboratory of Coordination Chemistry, Nanjing University, Nanjing, Jiangsu, 210023, P. R. China

*Corresponding authors (emails huanpangchem@hotmail.com, panghuan@yzu.edu.cn (H. Pang))

Table of Contents

Chemicals and Synthesis

Materials and instruments:

$Co(NO_3)_2·6H_2O$, 2-Methylimidazole (2-MeIM), cetyltrimethylammonium bromide (CTAB), HCl, and HF were bought from Aladdin Industrial Corporation. Titanium Aluminum Carbide (Ti_3AlC_2) was purchased from Laizhou Kai Kai Ceramic Materials Co., Ltd.

Synthesis of 2D MXene nanosheets

2D MXene nanosheets were obtained following a similar process in previous reports.[1] 1 g Ti_3AlC_2 was added to the etchant solution, consisting of 6 mL HCl, 1 mL HF and 3 mL deionized water (DI water). The reaction was stirred at 400 rpm for 15 h at 41 °C. Then, the resultant was washed with DI water repeatedly until pH was neutral (4500 rpm, 5 min), and the accordion-liked MXene was obtained. Subsequently, 25 mL DI water containing 1.5 g of LiCl was added. After reaction for 2 h, the resultant was washed with DI water repeatedly (3500 rpm, 5 min) and delaminated manually shaking agitation and centrifugation to obtain MXene suspension.

Synthesis of 3D MXene@ZIF-67

MXene@ZIF-67 composite was obtained following a similar process in previous reports.[1] 292 mg $Co(NO_3)_2·6H_2O$ was dissolved in 10 mL DI water containing 5 mg CTAB. Then this solution was rapidly injected into 70 mL MXene aqueous solution containing 4.54 g 2-MeIM and stirred at room temperature for 20 min. The obtained products were washed with DI water followed by freeze-drying.

Synthesis of 3D MXene@CS-ZCH

Typically, 0.04 g MXene@ZIF-67 powders were dispersed in 50 mL ethanol and stirred for 10 minutes. Simultaneously, 0.3 g $Co(NO_3)_2·6H_2O$ was dissolved in a

mixture of 50 mL ethanol and 50 μL DI water. Then, the $Co(NO_3)_2 \cdot 6H_2O$ solution was injected into the MXene@ZIF-67 solution rapidly with continuous stirring for 10 minutes. The products were washed with ethanol to obtain MXene@ CS-ZCH composite.

Synthesis of 3D MXene@YS-ZCH

Typically, 0.04 g MXene@ZIF-67 powders were dispersed in 50 mL ethanol and stirred for 10 minutes. Simultaneously, 0.3 g $Co(NO_3)_2 \cdot 6H_2O$ was dissolved in a mixture of 50 mL ethanol and 50 μL DI water. Then, the $Co(NO_3)_2 \cdot 6H_2O \cdot$solution was injected into the MXene@ZIF-67 solution rapidly with continuous stirring for 30 minutes. The obtained products were washed with ethanol thoroughly to obtain MXene@YS-ZCH composite.

Synthesis of 3D MXene@Ho-CH

Typically, 0.04 g MXene@ZIF-67 powders were dispersed in 50 mL ethanol and stirred for 10 minutes. Simultaneously, 0.3 g $Co(NO_3)_2 \cdot 6H_2O$ was dissolved in a mixture of 50 mL ethanol and 50 μL DI water. Then, the $Co(NO_3)_2 \cdot 6H_2O \cdot$solution was injected into the MXene@ZIF-67 solution rapidly with continuous stirring for 24 hours. The obtained products were washed with ethanol thoroughly to obtain Mxene@Ho-ZCH composite.

Synthesis of 3D cubic ZIF-67

Cubic ZIF-67 was obtained following a similar process in previous reports.[1] 292 mg $Co(NO_3)_2 \cdot 6H_2O$ was dissolved in 10 mL DI water containing 5 mg CTAB. Then this solution was rapidly injected into 70 mL DI water containing 4.54 g 2-MeIM and stirred at room temperature for 20 min. The obtained products were washed with DI water followed by freeze-drying.

Synthesis of CS-ZCH

Typically, 0.04 g cubic ZIF-67 powders were dispersed in 50 mL ethanol and stirred for 10 minutes. Simultaneously, 0.3 g $Co(NO_3)_2 \cdot 6H_2O$ was dissolved in a mixture of 50 mL ethanol and 50 μL DI water. Then, the $Co(NO_3)_2 \cdot 6H_2O$ solution was injected into the ZIF-67 solution rapidly with continuous stirring for 10 minutes. The products were washed with ethanol to obtain CS-ZCH.

Synthesis of 3D YS-ZCH

Typically, 0.04 g cubic ZIF-67 powders were dispersed in 50 mL ethanol and stirred for 10 minutes. Simultaneously, 0.3 g $Co(NO_3)_2 \cdot 6H_2O$ was dissolved in a mixture of 50 mL ethanol and 50 μL DI water. Then, the $Co(NO_3)_2 \cdot 6H_2O$ solution was injected into the ZIF-67 solution rapidly with continuous stirring for 2 h. The products were washed with ethanol to obtain YS-ZCH.

Synthesis of 3D Ho-CH

Typically, 0.04 g cubic ZIF-67 powders were dispersed in 50 mL ethanol and stirred for 10 minutes. Simultaneously, 0.3 g $Co(NO_3)_2 \cdot 6H_2O$ was dissolved in a mixture of 50 mL ethanol and 50 μL DI water. Then, the $Co(NO_3)_2 \cdot 6H_2O$ solution was injected into the ZIF-67 solution rapidly with continuous stirring for 6 h. The products were washed with ethanol to obtain Ho-CH.

Characterization

The detailed microstructures and morphology were observed by field emission scanning electron microscopy (FE-SEM, Zeiss-Supra55) under the acceleration voltage of 5.0 kV) and transmission electron microscopy (TEM, JEM-2100 instrument). High-resolution TEM (HRTEM) images, selected area electron

diffraction (SAED) images, and elemental mapping were captured on a Tecnai G2 F30 at an acceleration voltage of 300 kV. The crystal phase of the as-synthetized products was performed by X-ray diffraction (XRD) on a Bruker D8 Advanced X-ray Diffractometer (Cu-Kα radiation: λ = 0.15406 nm). Fourier transform infrared (FT-IR) spectra were supplied to characterize their information of chemical bonds or functional groups on a Cary 610/670. The specific surface area was obtained from the N_2 adsorption/desorption isotherms and was calculated by the Brunauer-Emmett-Teller (BET) method on JW-BK200. The surface composition and valence states were analyzed by X-ray photoelectron spectra (XPS) on a Thermo Scientific ESCALAB 250 apparatus.

Electrochemical measurements

Electrochemical tests with a three-electrode system

For the three-electrode system, the working electrode was obtained by mixing the active materials, acetylene black, and polytetrafluoroethylene (PTFE), at a weight ratio of 80 : 15 : 5. Then, a few drops of isopropanol were added to the above mixture and coated on nickel foam (1×1 cm^{-2}, current collector), which was following drying and pressed into a thin foil at a pressure of 8~10 MPa. The typical mass loading of the electrode material was 1.0~1.5 mg. The reference and counter electrodes were Hg/HgO (3.0 M KOH) and Pt wire, respectively. The cyclic voltammetry (CV), galvanostatic-charge discharge (GCD), and electrochemical impedance spectra (EIS) were tested on a CHI 760E electrochemical workstation in 3.0 M KOH. The specific capacitance (C) was calculated according to the following equation:

$$C = \frac{\int I\,dt}{m\,\Delta V} \quad \text{(S1)}$$

$$C = \frac{I\,\Delta t}{m\,\Delta V} \quad \text{(S2)}$$

here, I represents discharge current (A), Δt represents discharge time (s), m represents the mass of electroactive components (g), and ΔV represents potential window (V).

Evaluations with a two-electrode asymmetric supercapacitor

As for the asymmetrical supercapacitor, Mxene@Ho-CH and AC were used as the positive electrode and negative electrode, respectively. The Mxene@Ho-CH (or AC), acetylene black, and PTFE were milled according to the above proportions and coated on nickel foam. The mass ratio of the electrode was determined by balancing the charges stored in each electrode. Generally, the charges stored by positive and negative electrodes can be calculated by $q_+ = C_+ \times \triangle E_+ \times m_+$, and $q_- = C_- \times \triangle E_- \times m_-$, where C_+/C_- is the specific capacitance of the positive/negative electrode (F g^{-1}); $\triangle E$ represents the potential range (V); m_+/m_- is the weight of the active material in positive/negative electrode (g); The charges are balanced by the equation of $q_+ = q_-$, where q_+/q_- represents the charges stored in the positive/negative electrode. Therefore, $m_+/m_- = C_- \times \triangle E_-/C_+ \times \triangle E_+$, the mass ratio between the negative and positive electrodes was set to 4:1. The typical mass loading of the active material in the positive electrode was 1.0~1.5 mg. The electrochemical tests of CV and GCD were also tested on a CHI 760E electrochemical workstation in 3.0 M KOH. The areal specific capacitance (mF cm^{-2}) was calculated according to the following equations:

$$C = \frac{\int I\,dt}{A\,\Delta V} \quad \text{(S3)}$$

$$C = \frac{I\,\Delta t}{A\,\Delta V} \quad \text{(S4)}$$

here, I represents discharge current (A), Δt represents discharge time (s), A represents the surface area of the electrode deposited or coated with activate materials (cm^2), and ΔV represents potential window (V).

The power density (P, W cm^{-2})/energy density (E, Wh cm^{-2}) was calculated according to the following equations:

$$E = \frac{C\,\Delta V^2}{2} \quad \text{(S5)}$$

$$P = \frac{E}{\Delta t} \quad \text{(S6)}$$

Results and discussion

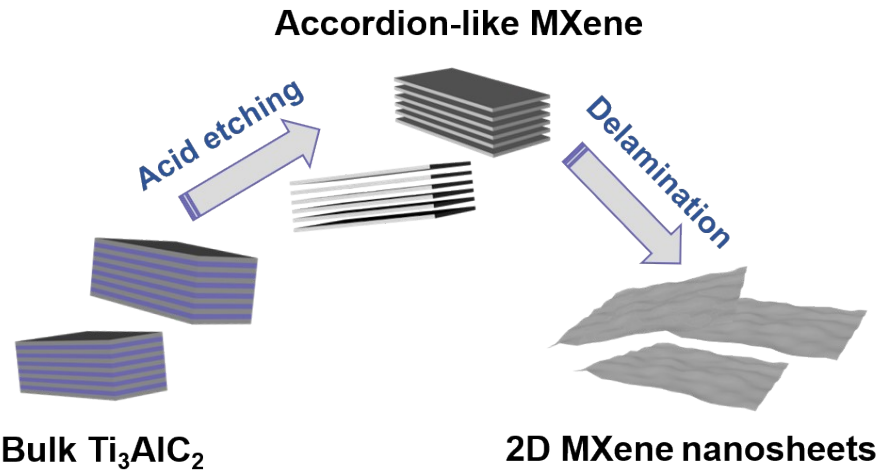

Scheme S1. Schematic of the synthesis of 2D MXene nanosheets.

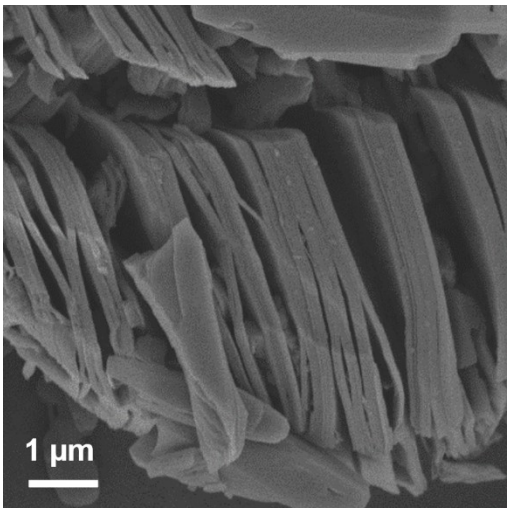

Figure S1. SEM image of accordion-like MXene.

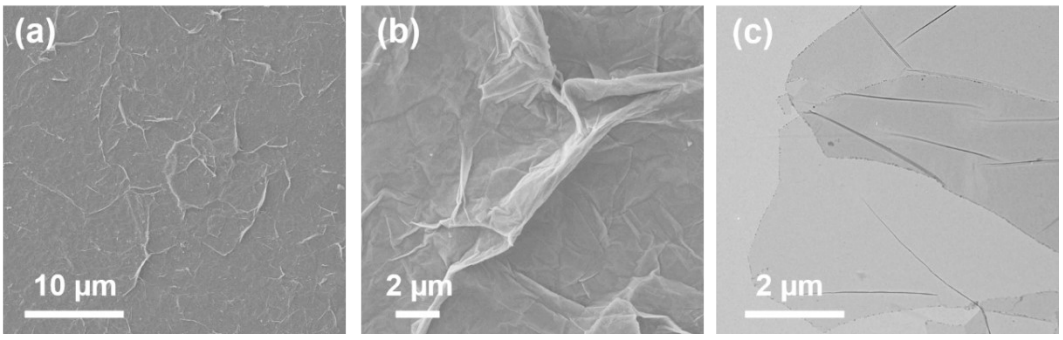

Figure S2. (a, b) SEM images and (c) TEM image of 2D MXene nanosheets.

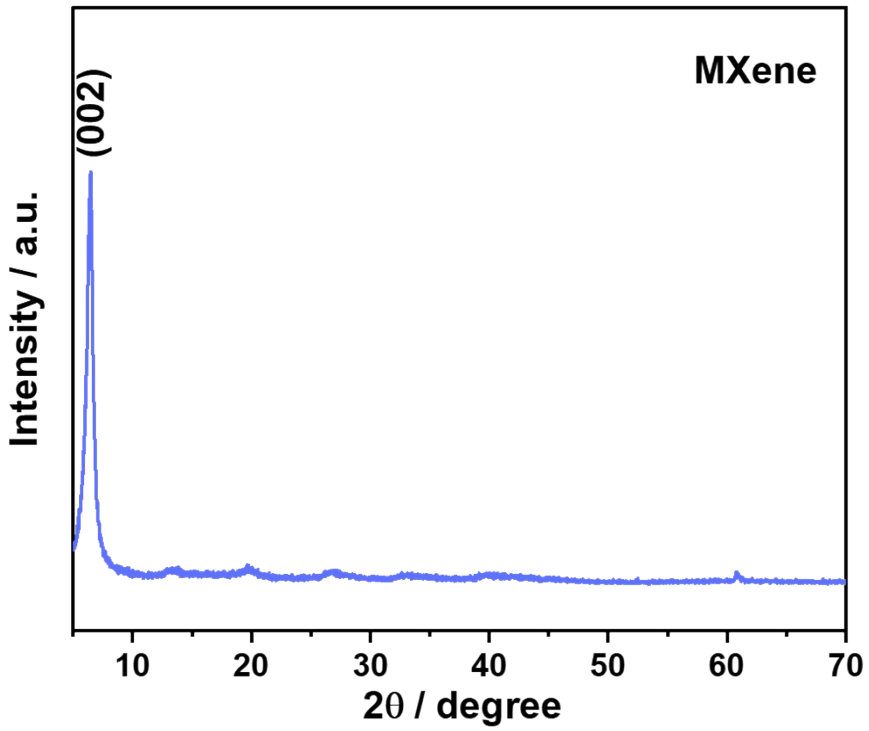

Figure S3. XRD of MXene.

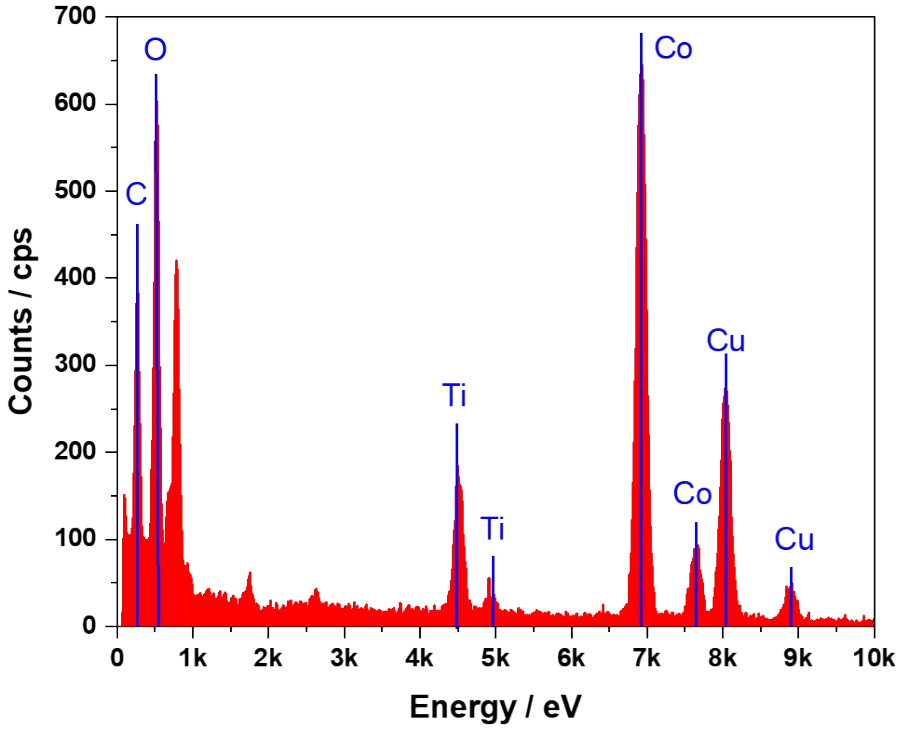

Figure S4. Energy-dispersive X-ray spectroscopy spectroscopy of Mxene@Ho-CH.

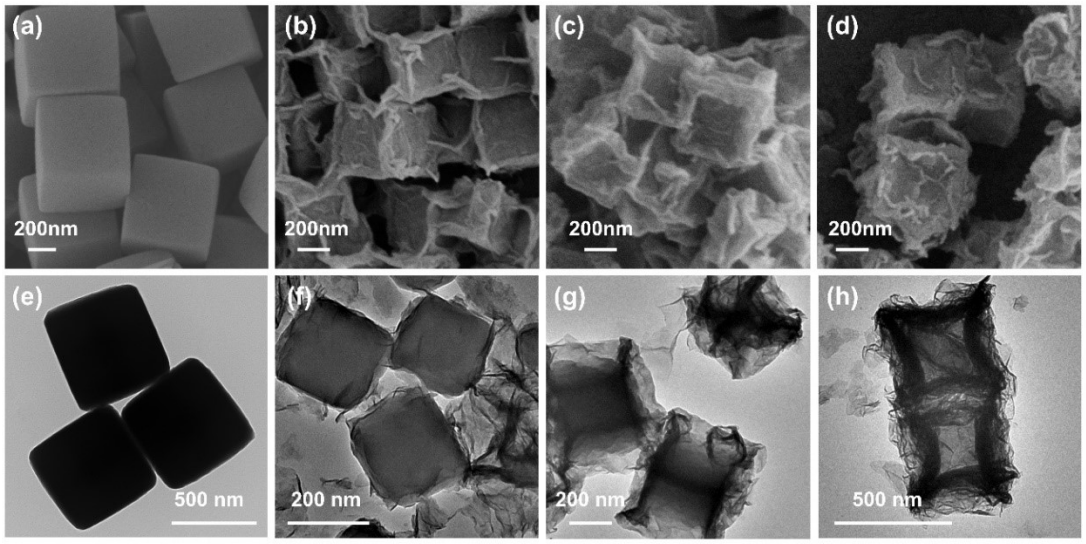

Figure S5. (a-d) SEM, (e-h) and TEM images of ZIF-67, CS-ZCH, YS-ZCH, and Ho-CH,respectively.

It could be seen that the surface of ZIF-67 is smooth without any wrinkles before alcoholization (Figure S5a, e). For CS-ZCH, the size of ZIF-67 nucleus begins to decrease. Meanwhile, a small amount of Co,Co-LDH nanosheets are uniformly coated on the surface of ZIF-67, forming a clear CS structure (Figure S5b, f). Further, the size of ZIF-67 nucleus continues to decrease, and the shell of Co,Co-LDH and core of ZIF-67 are separated (Figure S5c, g). Finally, ZIF-67 underwent CS and YS stages and was completely decomposed into Ho-CH (Figure S5d, h).

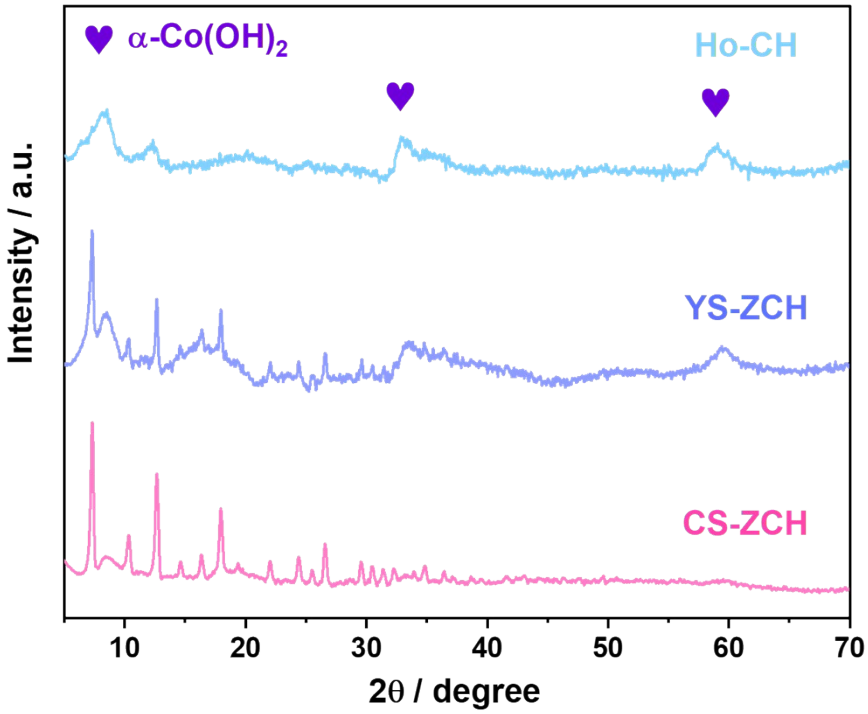

Figure S6. XRD of CS-ZCH, YS-ZCH, and Ho-ZCH.

For CS-ZCH, a small amount of Co,Co-LDH nanosheets were adsorbed on ZIF-67. Therefore, the XRD spectrum of CS-ZCH shows an obvious ZIF-67 phase (Figure 2a, gray), and it is difficult to observe the weak diffraction peak of *a*-$Co(OH)_2$. But as the reaction time increased, the peak of ZIF-67 began to weaken. Meanwhile, the peaks at 32.86 and 59.06° in XRD spectra confirmed the existence of the *a*-$Co(OH)_2$ phase (JCPDS No. 46-0605).[2]

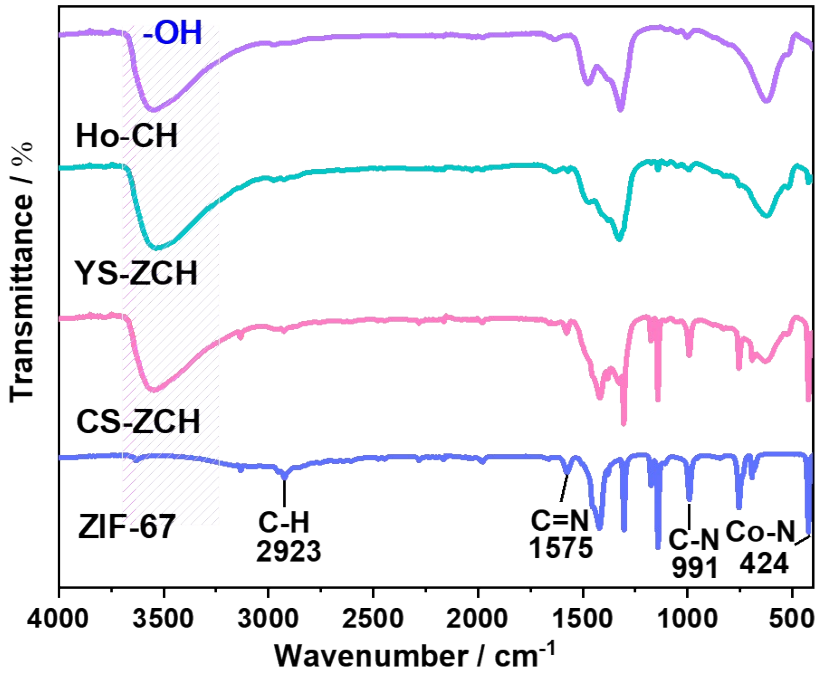

Figure S7. FT-IR spectra of ZIF-67, CS-ZCH, YS-ZCH, and Ho-ZCH.

For ZIF-67, the stretching vibration at 2923 cm^{-1} can be attributed to the C−H bond in methyl. The peaks at 991 and 1575 cm^{-1} correspond to the vibrations of C−N and C=N.[3–5] In addition, the characteristic peak of Co−N at 424 cm^{-1} was observed. For CS-ZCH, YS-ZCH, and Ho-CH, it could be seen that the diffraction peak of ZIF-67 gradually weakens, and apparent broad peak appears at ~3500 cm^{-1}, corresponding to −OH.

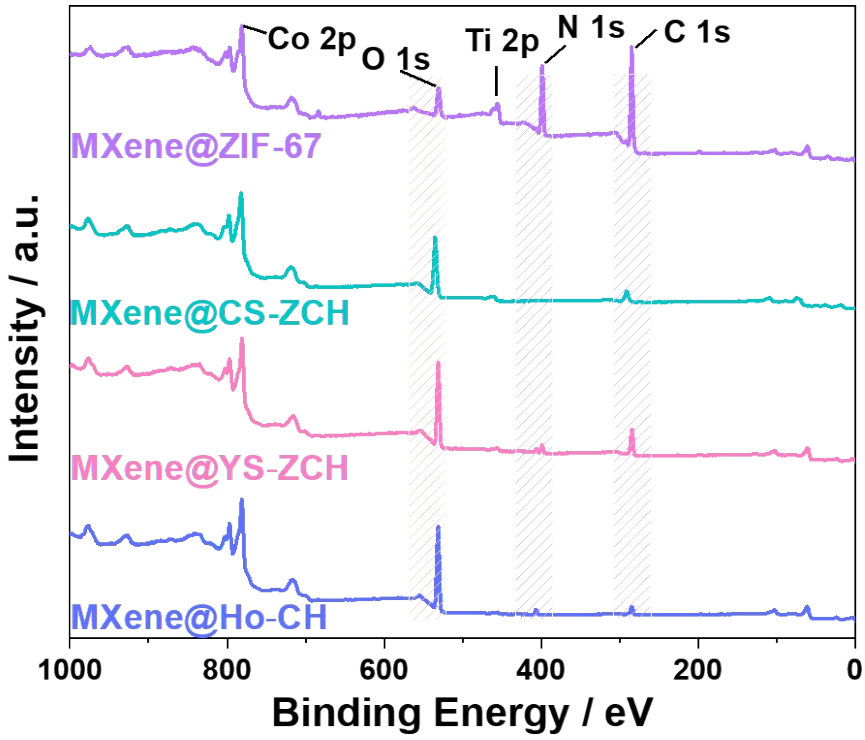

Figure S8. Survey XPS spectra of MXene@ZIF-67, MXene@CS-ZCH, MXene@YS-ZCH, and Mxene@Ho-ZCH.

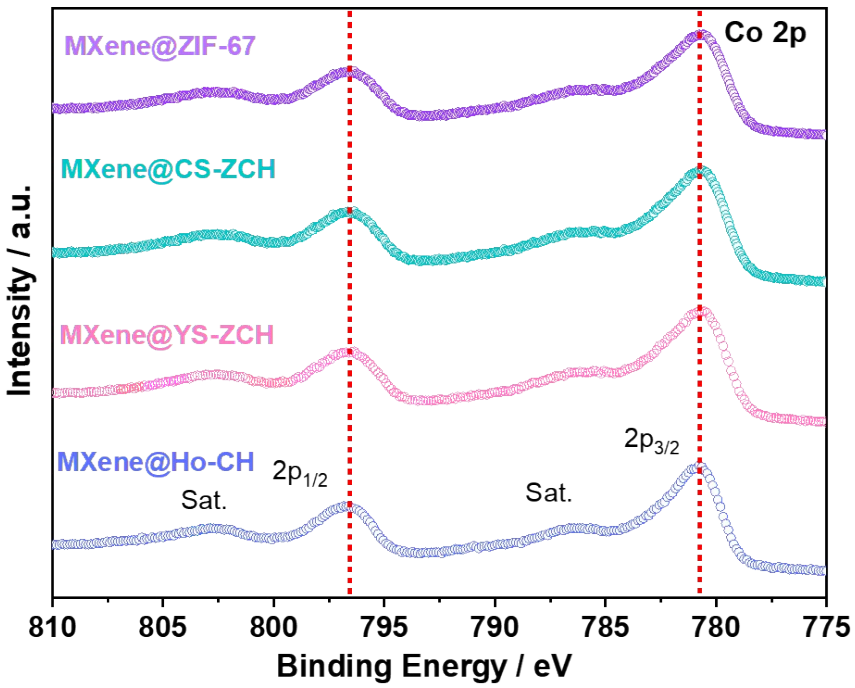

Figure S9. Co 2p XPS spectra of MXene@ZIF-67, MXene@CS-ZCH, MXene@YS-ZCH, and Mxene@Ho-ZCH.

Table S1 The detailed C 1s XPS analyses of MXene@ZIF-67, MXene@CS-ZCH, MXene@YS-ZCH, and MXene@Ho-ZCH.

Binding Energy / eV				Bond type
MXene@ZIF-67	**MXene@CS-ZCH**	**MXene@YS-ZCH**	**MXene@Ho-ZCH**	
281.09 eV	281.71	281.76	281.93	C−Ti
284.80	284.80	284.80	284.80	C−C
285.79	285.88	286.01	285.68	C−N
--	288.95	288.83	288.73	C=O

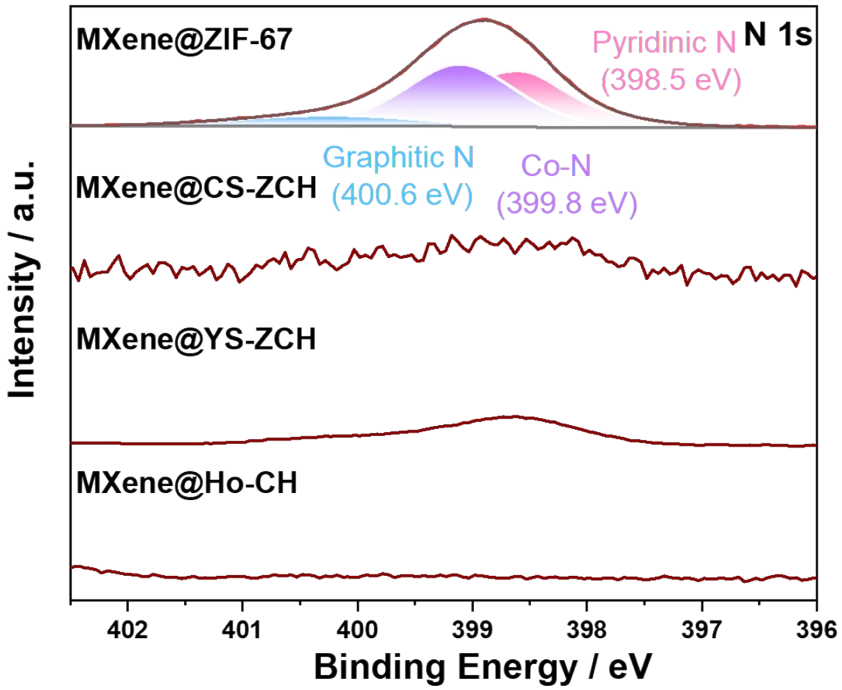

Figure S10. N 1s XPS spectra of MXene@ZIF-67, MXene@CS-ZCH, MXene@YS-ZCH, and Mxene@Ho-ZCH.

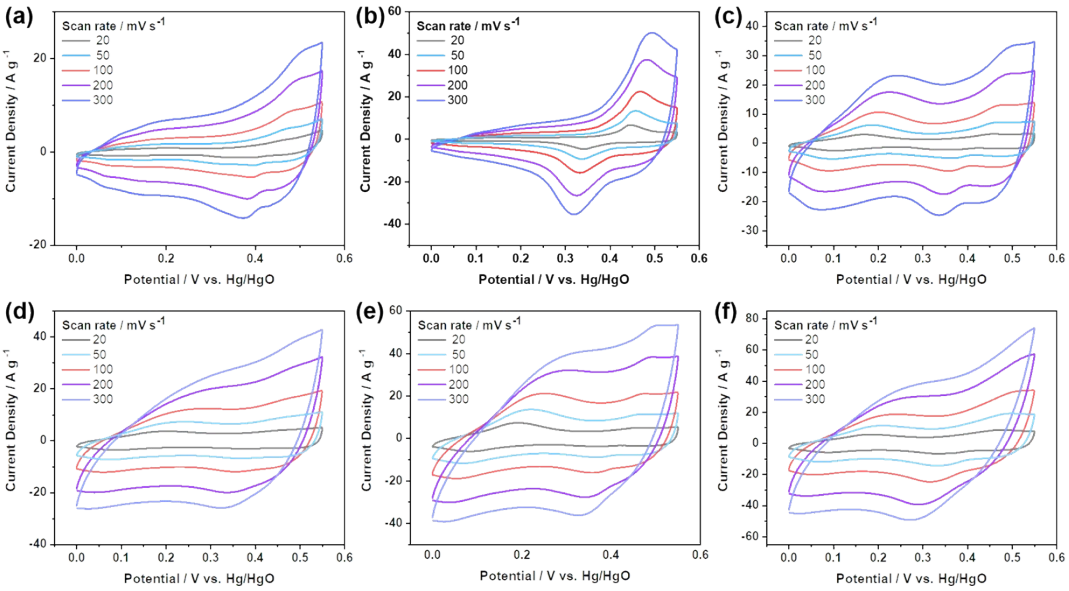

Figure S11. CV curves of (a) ZIF-67, (b) MXene@ZIF-67, (c) Ho-ZCH, (d) MXene@CS-ZCH, (e) MXene@YS-ZCH, and (f) Mxene@Ho-ZCH.

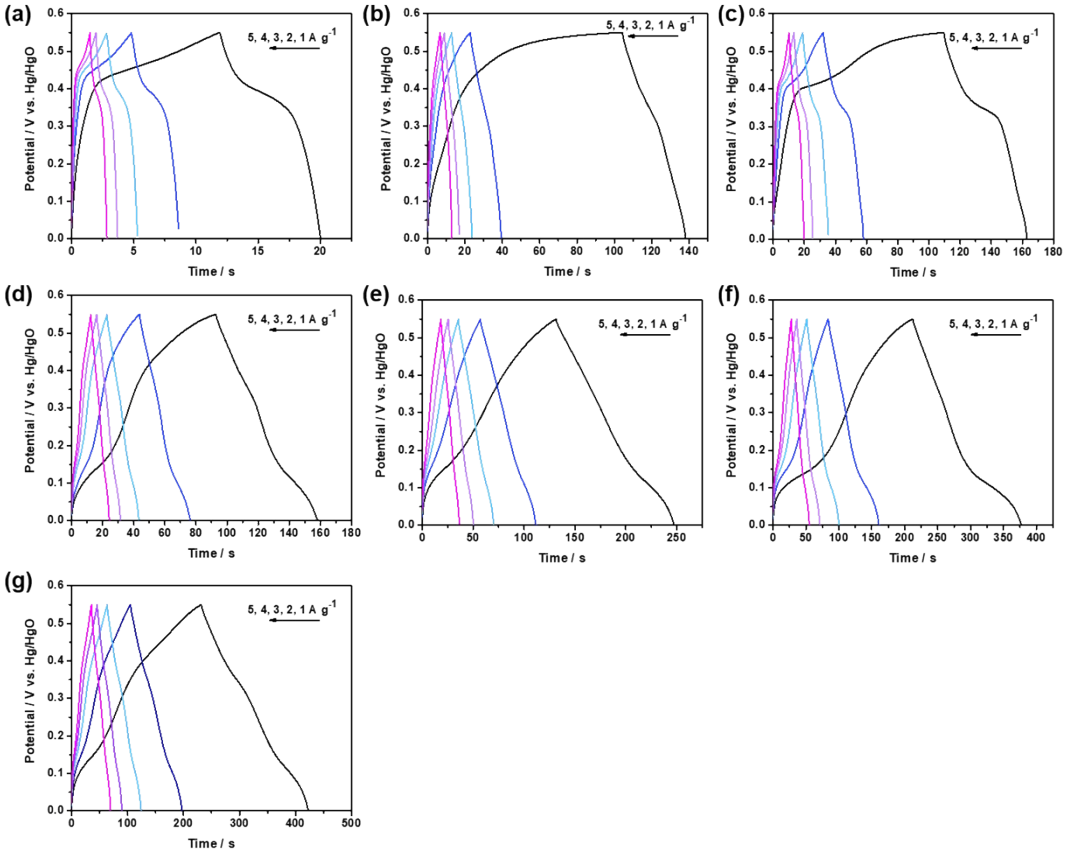

Figure S12. GCD curves of (a) MXene, (b) ZIF-67, (c) MXene@ZIF-67, (d) Ho-ZCH, (e) MXene@CS-ZCH, (f) MXene@YS-ZCH, and (g) Mxene@Ho-ZCH.

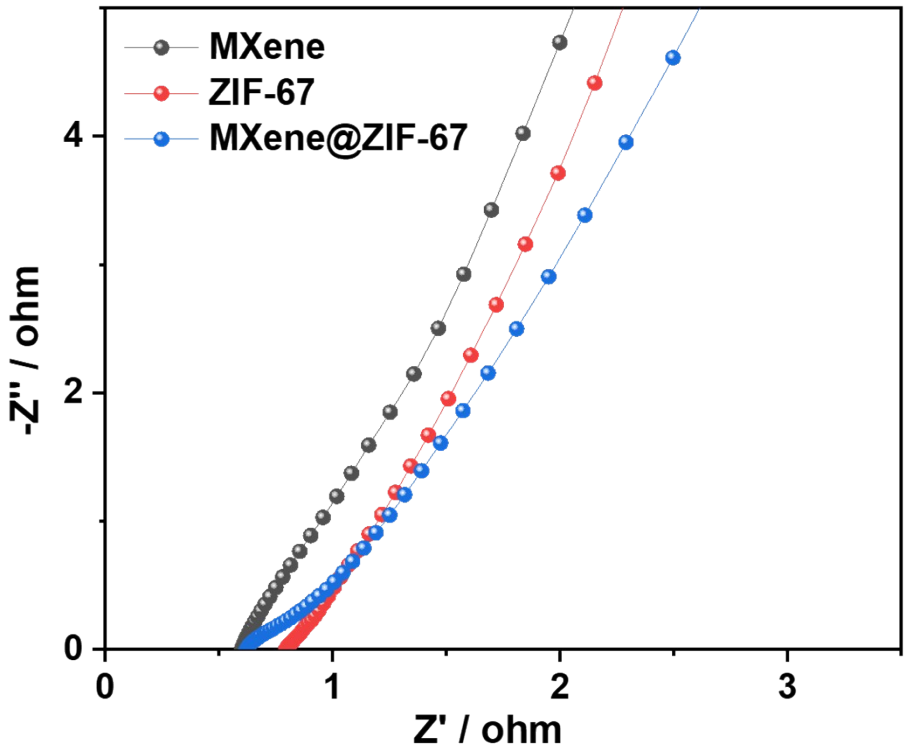

Figure S13. Nyquist plots of MXene, ZIF-67, and MXene@ZIF-67.

According to the Nyquist plots, MXene exhibits the lowest electrolyte resistance. Moreover, the electrolyte resistance of pure ZIF-67 electrode is larger than that of MXene@ZIF-67, manifesting that the presence of MXene as a conductive substrate improves the electrical conductivity of the composite.

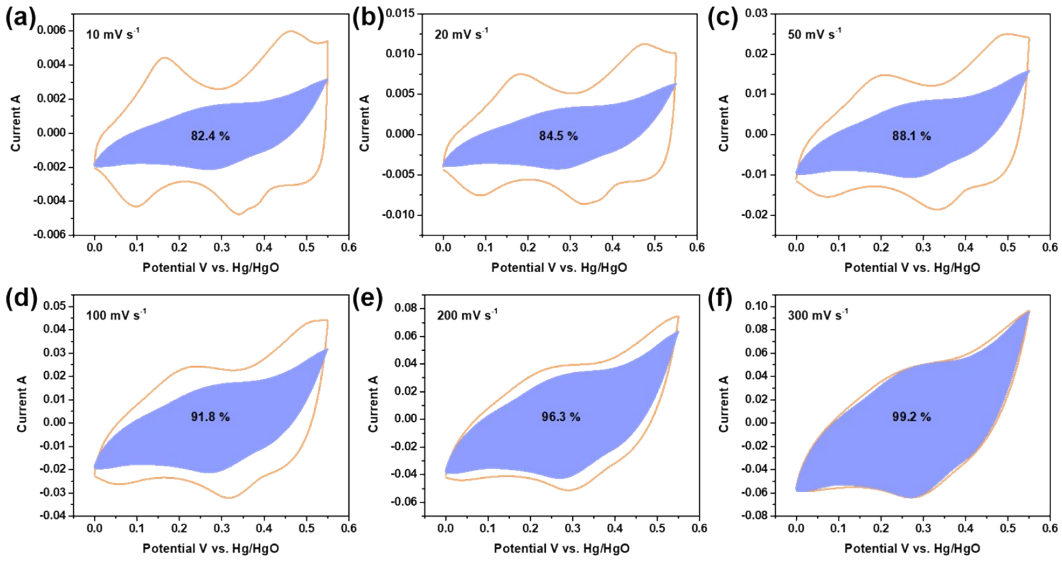

Figure S14. Separation of capacitive (interior region) and diffusion-controlled (exterior region) contribution at different scanning rates.

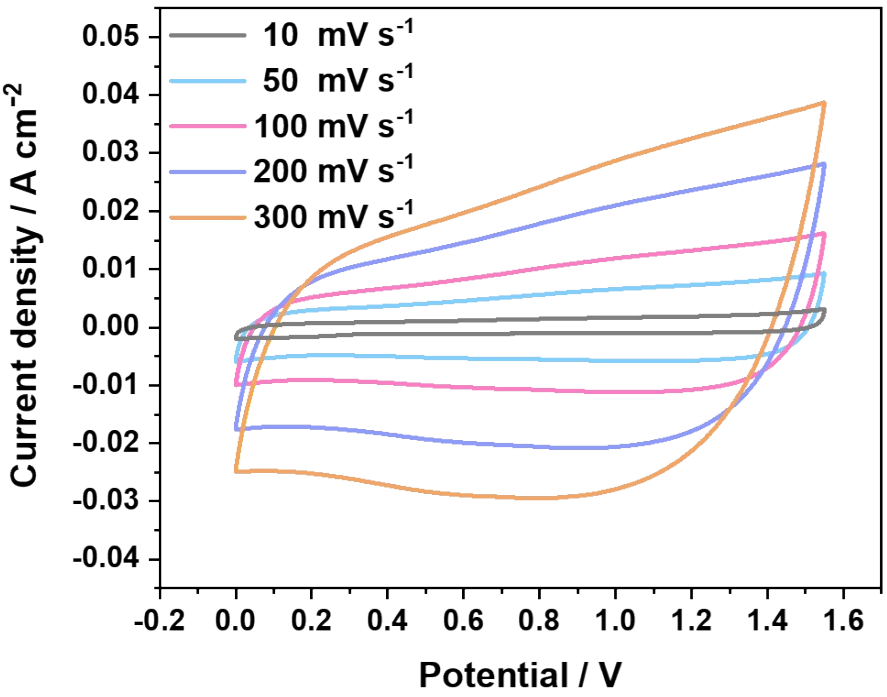

Figure S15. CV curves of Mxene@Ho-ZCH//AC at various scan rates in a two-electrode system in 3.0 M KOH.

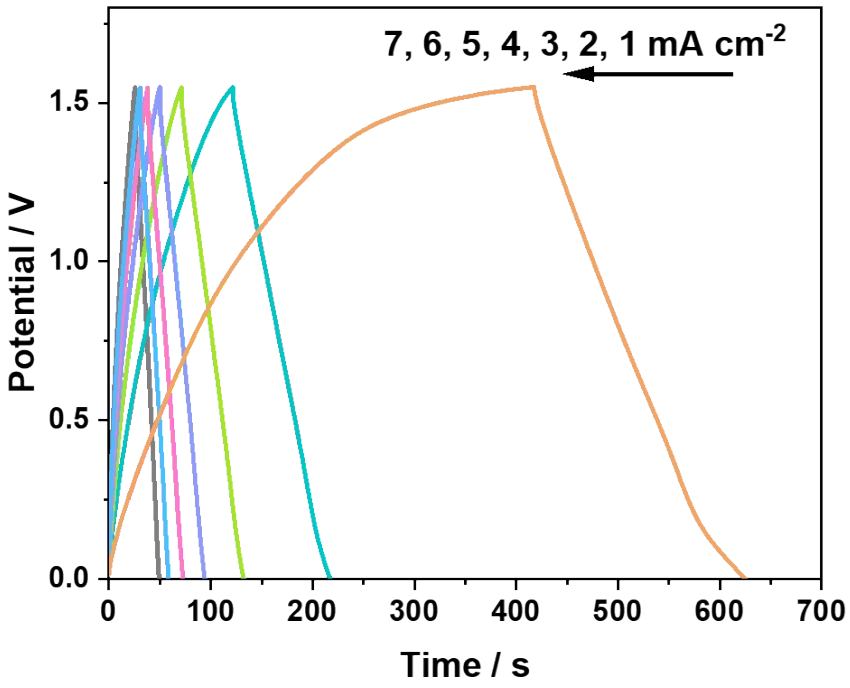

Figure S16. GCD curves of Mxene@Ho-ZCH//AC in a two-electrode system in 3.0 M KOH.

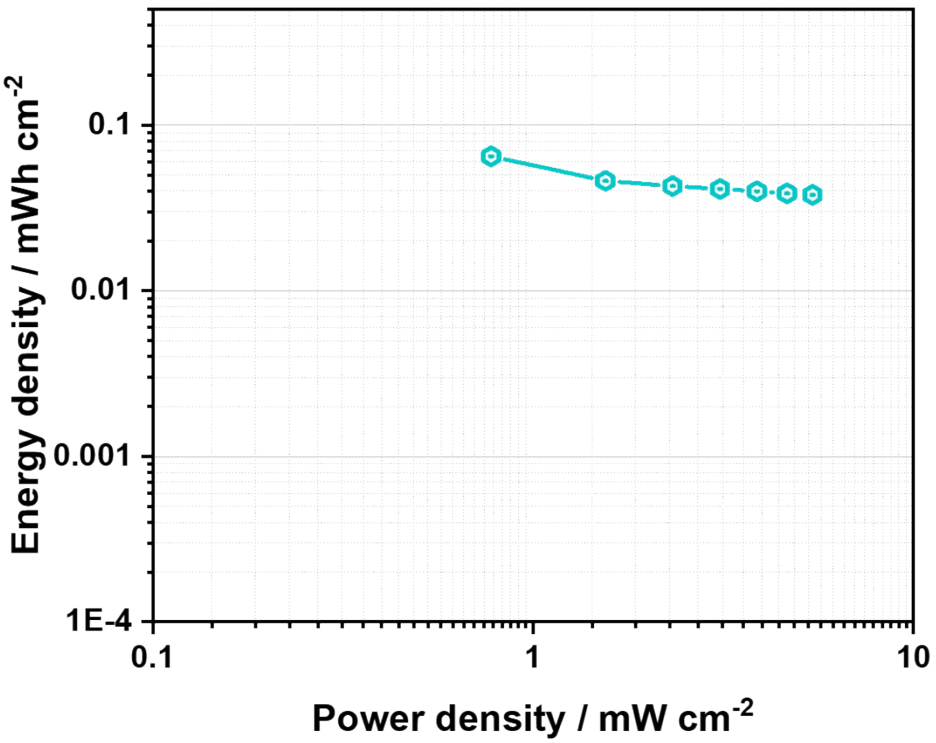

Figure S17. Energy density versus power density plots of Mxene@Ho-ZCH//AC.

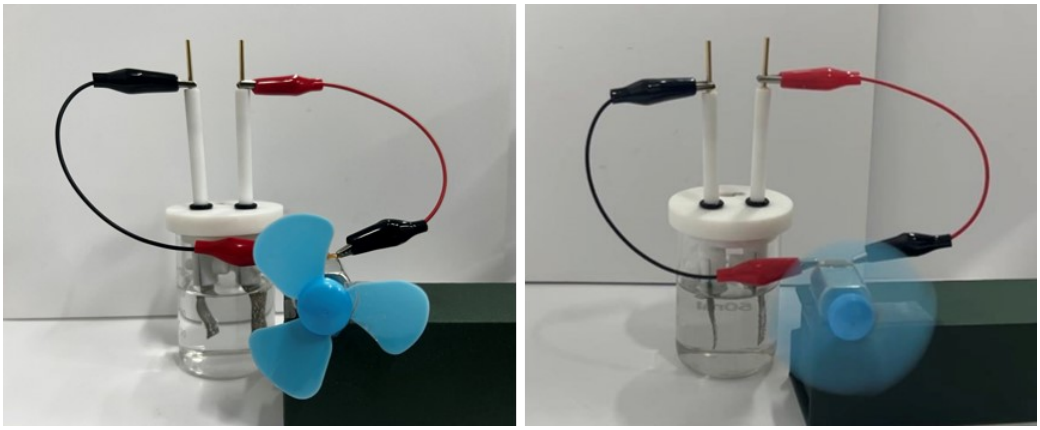

Figure S18. Optical image of motor powered by Mxene@Ho-ZCH//AC.

Reference

1 C. Liu, Y. Bai, W. Li, F. Yang, G. Zhang and H. Pang, In Situ Growth of Three-Dimensional MXene/Metal–Organic Framework Composites for High-Performance Supercapacitors, *Angew. Chem. Int. Ed.*, 2022, **61**, e202116282.

2 C. Liu, Y. Bai, J. Wang, Z. Qiu and H. Pang, Controllable Synthesis of Ultrathin Layered Transition Metallic Hydroxide/Zeolitic Imidazolate Framework-67 Hybrid Nanosheets for High-Performance Supercapacitors, *J. Mater. Chem. A*, 2021, **9**, 11201–11209.

3 U. P. N. Tran, K. K. A. Le and N. T. S. Phan, Expanding applications of metal-organic frameworks: Zeolite imidazolate framework zif-8 as an efficient heterogeneous catalyst for the knoevenagel reaction, *ACS Catal.*, 2011, **1**, 120–127.

4 S. Wu, W. Wang, Y. Fang, X. Kong and J. Liu, Efficient Friedel–Crafts acylation of anisole over silicotungstic acid modified ZIF-8, *Reac. Kinet. Mech. Cat.*, 2017, **122**, 357–367.

5 Y. Zhang and S.-J. Park, Facile construction of MoO_3@ZIF-8 core-shell nanorods for efficient photoreduction of aqueous Cr (VI), *Appl. Catal. B Environ.*, 2019, **240**, 92–101.